ANZIAM J. **63** (2021), 228–248
doi:10.1017/S1446181121000286

SPECTRALLY ACCURATE OPTION PRICING UNDER THE TIME-FRACTIONAL BLACK–SCHOLES MODEL

GERALDINE TOUR[1], NAWDHA THAKOOR[1] and DÉSIRÉ YANNICK TANGMAN[1]✉

(Received 29 April, 2020; accepted 7 April, 2021; first published online 25 August, 2021)

Abstract

We propose a Legendre–Laguerre spectral approximation to price the European and double barrier options in the time-fractional framework. By choosing an appropriate basis function, the spectral discretization is used for the approximation of the spatial derivatives of the time-fractional Black–Scholes equation. For the time discretization, we consider the popular $L1$ finite difference approximation, which converges with order $O((\Delta\tau)^{2-\alpha})$ for functions which are twice continuously differentiable. However, when using the $L1$ scheme for problems with nonsmooth initial data, only the first-order accuracy in time is achieved. This low-order accuracy is also observed when solving the time-fractional Black–Scholes European and barrier option pricing problems for which the payoffs are all nonsmooth. To increase the temporal convergence rate, we therefore consider a Richardson extrapolation method, which when combined with the spectral approximation in space, exhibits higher order convergence such that high accuracies over the whole discretization grid are obtained. Compared with the traditional finite difference scheme, numerical examples clearly indicate that the spectral approximation converges exponentially over a small number of grid points. Also, as demonstrated, such high accuracies can be achieved in much fewer time steps using the extrapolation approach.

2020 *Mathematics subject classification*: 65M70.

Keywords and phrases: spectral element discretization, option pricing, time-fractional Black–Scholes equation.

1. Introduction

Apart from providing useful instruments for the study of important phenomena in different fields of engineering and science, fractional order derivatives have also been successfully applied in the financial field. The classical Black–Scholes [1] equation is one of the most powerful option pricing tools related to most of the

[1]Department of Mathematics, University of Mauritius, Reduit, Mauritius
e-mail: dine2409@hotmail.com, n.thakoor@uom.ac.mu, y.tangman@uom.ac.mu

models used for quantitative financial calculations. Generalizing the Black–Scholes equation to a fractional order can lead to the time-fractional and space-fractional Black–Scholes equations. Regarding option pricing under the modified Black–Scholes equation, different investigations have been sought, both in analytical and numerical settings.

Analytical solutions for the European options under the Black–Scholes fractional model have been derived previously [7, 19, 32]. The double barrier options were analytically priced by Chen et al. [9]. However, these formulae are complicated and difficult to evaluate. As such, practical numerical approximate solutions for the Black–Scholes fractional order models were provided. An implicit finite-difference technique was considered for option pricing by Song and Wang [31]. Chen et al. [8] proposed a predictor–corrector approach to price the American options in the fractional framework. For the time-fractional Black–Scholes model, finite-difference approximations were also considered by Koleva and Vulkov [20]. The effect of trend memory in financial option pricing was described by Farhadi et al. [14] using the time-fractional Black–Scholes equation. Chen et al. [3] recently considered an operator splitting method for the evaluation of American options under the same model. Zhang et al. [37] proposed a new fractional option pricing model employing both time- and space-fractional derivatives based on the finite moment log-stable (FMLS) model. The time-fractional Black–Scholes model was considered by Golbabai et al. [16] using radial basis functions (RBFs) in the spatial sense and a finite-difference scheme for time. More recently, a two-dimensional fractional partial differential equation (FPDE) has been established, based on the two-dimensional FMLS model for option pricing [10]. Recently, several researchers [6, 17, 23, 25, 27–29] have investigated the problem of option pricing under the Black–Scholes fractional framework or the generalized Black–Scholes equation. Such low-order convergence in both space and time implies that we need a lot of computational nodes in both dimensions to reach reasonable accuracies.

In this paper, we consider the time-fractional Black–Scholes model with a spectral element discretization in space. The approximation of the fractional time derivative is usually based on the finite-difference approach. The most common difference approximation of the time-fractional derivative is the $L1$ method, which is an implicit numerical scheme with accuracy proven to be of order $2-\alpha$ for twice continuously differentiable functions [22]. Zhang et al. [38] considered the $L1$ approximation [22] to approximate the Black–Scholes time-fractional derivative for the European options with a second-order finite-difference scheme for the spatial discretization. To improve their results [38], De Staelen and Hendy [12] later considered a fourth-order scheme in space with the same $2-\alpha$ scheme in time for the valuation of double barrier options under the time-fractional Black–Scholes model. However, the $L1$ scheme exhibits only a first-order rate of convergence in time for FPDEs with nonsmooth initial data or without a source term, as proven in [18, 33, 34]. This is also observed for option pricing problems for which the payoffs are all nonsmooth; there is no sourcing term and the solutions have low regularity near maturity. Moreover, Cen et al. [2]

https://doi.org/10.1017/S1446181121000286 Published online by Cambridge University Press

obtained a first-order convergence in time under the time-fractional Black–Scholes model for the European call options. We further note that the main results obtained in the papers mentioned earlier [12, 16, 38] are only valid for payoff functions that are smooth enough, which exclude the European or even the double barrier options.

To increase the temporal accuracy of the solution obtained using the $L1$ approximation [15], we propose to use the Richardson extrapolation approach. Since it is a well-known technique, this approach can be used to increase the speed and rate of convergence of any numerical scheme with a known order of convergence. As such, we employ the Richardson extrapolation approach with prior knowledge of the rate of convergence of the $L1$ discretization to obtain higher accuracy numerical solutions for the European and barrier options. We also consider a spectral approximation for the spatial discretization. More specifically, to approximate the spatial derivatives, we consider the spectral element method which retains exponential convergence. Splitting the computational domain into two parts, the Legendre basis functions are used in the finite sub-domain and the infinite sub-domain is expanded using the Laguerre functions [30], all with associated Gauss-quadrature rules [26, 30]. Spectral approximations for space discretizations of fractional diffusion equations is not new as it can be seen in several works [4, 5, 21, 22]. However, to the best our knowledge, the spectral element method has not been applied in option pricing under the time-fractional Black–Scholes model. Since the approximations over each element are almost separated, the spectral element method allows us to use a small number of grid nodes to attain spectral accuracy in space, such that linear systems of moderate sizes are solved at each time step. As shown later in our numerical experiments, highly accurate results are obtained using both the spectral approximation and the Richardson extrapolation methods. Exponential convergence is achieved with much fewer grid points compared with the finite-difference method. This considerably improves the computational time of the numerical schemes.

This paper is outlined as follows. In Section 2, we describe the pricing equation along with the initial and boundary conditions for pricing European and barrier options under the time-fractional Black–Scholes model. In Section 3, we review the finite-difference approximation of the time-fractional derivative, and the Legendre–Laguerre approximation is described in Section 4. In Section 5, we describe the Richardson extrapolation approach. The computational efficiency of the spectral element method and the Richardson extrapolation scheme is shown by our numerical results in Section 6, and concluding remarks are given in Section 7.

2. Time-fractional Black–Scholes model

We let $v(S, \tau)$ denote the value of a European put option price, with S being the underlying asset and $\tau = T - t$ representing the time remaining for maturity T.

https://doi.org/10.1017/S1446181121000286 Published online by Cambridge University Press

Under the time-fractional Black–Scholes model, $v(S,\tau)$ satisfies

$$\mathcal{D}_\tau^\alpha v(S,\tau) = \mathcal{L}v(S,\tau), \quad S \in \Omega = [0,\infty), \quad 0 < \tau \le T, \tag{2.1}$$

where

$$\mathcal{L} = \frac{1}{2}\sigma^2 S^2 \frac{\partial^2}{\partial S^2} + (r-\delta)S\frac{\partial}{\partial S} - r,$$

subject to the conditions

$$\begin{aligned} v_0 &= v(S,0) = \max(K-S,0),\\ v(0,\tau) &= Ke^{-r\tau} - Se^{-\delta\tau},\\ \lim_{S\to+\infty} v(S,\tau) &= 0, \end{aligned}$$

where r, σ and δ are the risk-free interest rate, volatility and the continuous dividend yield, respectively. The fractional derivative in (2.1), also known as the Caputo derivative, is defined as

$$\mathcal{D}_\tau^\alpha v(S,\tau) = \frac{1}{\Gamma(1-\alpha)}\int_0^\tau \frac{\partial v(S,\eta)}{\partial \eta}(\tau-\eta)^{-\alpha}\,d\eta, \quad 0<\alpha<1. \tag{2.2}$$

Among the most common exotic options traded in equity option markets are the barrier options. We consider a double knock-out call barrier option which consists of a "down-and-out" and an "up-and-out" barrier option with lower barrier level B_l and upper barrier level B_u, respectively. The valuation problem being similar to that of a European call option, the boundary and initial conditions are given by

$$\begin{aligned} v_0 &= v(S,0) = \max(S-K,0), \quad B_l < S < B_u,\\ v(B_l,\tau) &= v(B_u,\tau) = 0. \end{aligned}$$

3. $L1$ approximation

The $L1$ method is the most common difference approximation of the time-fractional derivative [22]. Let $\tau_m = m\Delta\tau$, $m = 0,1,\ldots,M$, denote the temporal mesh, where $\Delta\tau = T/M$ represents one time step. Then, (2.2) can be rewritten as

$$\mathcal{D}_\tau^\alpha v(S,\tau_{m+1}) = \frac{1}{\Gamma(1-\alpha)}\sum_{j=0}^{m}\int_{\tau_j}^{\tau_{j+1}} \frac{\partial v(S,\eta)}{\partial \eta}(\tau_{m+1}-\eta)^{-\alpha}\,d\eta,$$

such that further simplifications lead to the discrete fractional differential operator $\mathcal{F}_\tau^\alpha$, defined by

$$\mathcal{F}_\tau^\alpha v(S,\tau_{m+1}) = \frac{1}{\Gamma(2-\alpha)}\sum_{j=0}^{m} b_j \frac{v(S,\tau_{m+1-j}) - v(S,\tau_{m-j})}{(\Delta\tau)^\alpha},$$

https://doi.org/10.1017/S1446181121000286 Published online by Cambridge University Press

where $b_j = (j+1)^{1-\alpha} - j^{1-\alpha}$ are the weights for $j = 0, 1, \ldots, m$. This yields

$$\mathcal{D}_\tau^\alpha v(S, \tau_{m+1}) = \mathcal{F}_\tau^\alpha v(S, \tau_{m+1}) + \varepsilon_{\Delta\tau}^{m+1},$$

where $\varepsilon_{\Delta\tau}^{m+1}$ is the truncation error. For smooth problems, the $L1$-based scheme has time convergence $O((\Delta\tau)^{2-\alpha})$ [22]. However, this scheme exhibits only first-order accuracy in time when solving FPDEs with nonsmooth initial data or without a source term [18, 33, 34]. The same phenomena are observed when solving for the European and barrier option pricing problems in the time-fractional framework, for which the payoffs are all nonsmooth, there is no sourcing term and the solutions have low regularity near maturity [2].

Using $\mathcal{F}_\tau^\alpha v(S, \tau_{m+1})$ as an approximation of $\mathcal{D}_\tau^\alpha v(S, \tau_{m+1})$, we have

$$\mathcal{F}_\tau^\alpha v^{m+1} = \mathcal{L} v^{m+1}, \tag{3.1}$$

for $m = 0, 1, \ldots, M-1$, where v^{m+1} is an approximation to $V(S, \tau_{m+1})$. Equation (3.1) can then be rewritten as

$$b_0 v^{m+1} - \Gamma(2-\alpha)\Delta\tau^\alpha \mathcal{L} v^{m+1} = b_0 v^m - \sum_{j=1}^{m-1} b_{j+1} v^{m-j} + \sum_{j=1}^{m} b_j v^{m-j}. \tag{3.2}$$

With $b_0 = 1$ and letting $\alpha_0 = \Gamma(2-\alpha)\Delta\tau^\alpha$, (3.2) can be rearranged such that

$$v^{m+1} - \alpha_0 \mathcal{L} v^{m+1} = (1 - b_1) v^m + \sum_{j=1}^{m-1} (b_j - b_{j+1}) v^{m-j} + b_m v^0. \tag{3.3}$$

Let $\mathcal{B}(\mathcal{L}) = H^1(\Omega) \cap H^2(\Omega)$, where $H^1(\Omega)$ and $H^2(\Omega)$ denote the usual Sobolev spaces with corresponding norms $\|\cdot\|_{H^1(\Omega)}$ and $\|\cdot\|_{H^2(\Omega)}$, respectively.

THEOREM 3.1. [35, Theorem 3.2] *Let $v(\tau_m)$ and v^m be the solutions of (2.1) and (3.3), respectively, and let $v_0 \in \mathcal{B}(\mathcal{L})$. Then, with $0 < \alpha < 1$ and the constant C positive,*

$$\|\bar{v}(\tau_m) - \bar{v}^m\|_{L_2(\Omega)} \leq C(\Delta\tau)\tau_m^{\alpha-1}\|v_0\|_{L_2(\Omega)}.$$

4. Legendre–Laguerre spectral method in space

We describe in this section the spectral element discretization in space of the time-fractional Black–Scholes equation (2.1). Before defining the weak formulation problem, we start with some basic notation. Consider the domain Ω with the Sobolev space,

$$H^m(\Omega) = \left\{ u \in L^2(\Omega),\ \frac{d^k u}{dx^k} \in L^2(\Omega),\ 0 \leq k \leq m \right\},$$

https://doi.org/10.1017/S1446181121000286 Published online by Cambridge University Press

where $L^2(\Omega)$ is the space of square integrable functions on Ω. The spaces $L^2(\Omega)$ and $H^m(\Omega)$ are equipped with inner products defined by

$$(u, v)_\Omega = \int_\Omega u(x)v(x)\,dx, \quad (u, v)_{m,\Omega} = \sum_{k=0}^{m} \int_\Omega \frac{d^k u}{dx^k}\frac{d^k v}{dx^k}\,dx,$$

respectively; and for any two functions $u, v \in L^2(\Omega)$, the corresponding norms are

$$\|v\|_{L^2(\Omega)} = (v, v)_\Omega^{1/2}, \quad \|v\|_{H^m(\Omega)} = (v, v)_{m,\Omega}^{1/2}.$$

In general, the entire domain is separated into several sub-domains depending on the smoothness of the solution in the different parts of the domain. Then different kinds of methods can be used accordingly in the different sub-domains. Generally, for the coupled Legendre–Laguerre spectral method, the interval $\Omega = [0, \infty)$ can be split, so that we let $\Omega_1 = [0, a]$ and $\Omega_2 = [a, \infty)$ for some $a > 0$. Then Ω_1 can be further partitioned into E nonoverlapping sub-domains, $\Omega_1^e = [a_{e-1}, a_e]$, $e = 1, 2, \ldots, E$, where a_e, $e = 0, 1, \ldots, E$ are the $E + 1$ points such that $0 = a_0 < a_1 < \cdots < a_E = a$. Within each sub-domain, the spectral representation will be established in a specific polynomial space. Over Ω_1, we use the Legendre polynomials $\{L_{n_1}, n_1 \geq 0\}$ which are orthogonal in the interval $[-1, 1]$ with unitary weight. Let $\mathbb{P}_{n_1}$ denote the space of all Legendre polynomials of degree at most n_1, then we can define the piecewise polynomial space

$$\mathbb{P}_{n_1,E}(\Omega_1) = \{u;\, u_{|\Omega_1^e} \in \mathbb{P}_{n_1}(\Omega_1^e),\, e = 1, \ldots, E\}.$$

Let $\{x_k, w_k\}_{k=0}^{n_1}$ be the set of the Gauss–Lobatto–Legendre [26] quadrature nodes and weights. Here, $\{x_k\}_{k=0}^{n_1}$ are the roots of the polynomial $L_{n_1+1}(x) - L_{n_1-1}(x)$, and the corresponding weights associated with the grid points are

$$w_k = \frac{2}{n_1(n_1 + 1)L_{n_1}^2(x_k)}, \quad k = 0, 1, \ldots, n_1.$$

Equivalent to the Lagrange interpolation polynomial, the Gauss–Lobatto–Legendre basis function, $\phi_k(x)$, is defined as

$$\phi_k(x) = \frac{L_{n_1+1}(x) - L_{n_1-1}(x)}{(2n_1 + 1)(x - x_k)L_{n_1}(x_k)}, \quad k = 0, 1, \ldots, n_1.$$

In Ω_2, we consider the stable Gauss–Radau–Laguerre basis functions [30]. The Laguerre polynomials $\{\mathcal{L}_{n_2}(x), n_2 \geq 0\}$ are orthogonal with respect to a weighting function $\omega(x) = e^{-x}$ on $[0, \infty)$. Since the weights decay very rapidly as n_2 increases, for stability, we consider the modified Laguerre polynomial

$$\hat{\mathcal{L}}_{n_2}(x) = e^{-x/2}\mathcal{L}_{n_2}(x), \quad n_2 \geq 0.$$

We then let $\hat{\mathbb{P}}_{n_2}(\Omega_2)$ be the space of the modified Laguerre polynomials of degree less than or equal to n_2. For the stable Gauss–Radau–Laguerre quadrature, with $\hat{x}_0 = 0$,

https://doi.org/10.1017/S1446181121000286 Published online by Cambridge University Press

$\{\hat{x}_k\}_{k=1}^{n_2}$ are the roots of $\partial_x \hat{\mathcal{L}}_{n_2+1}(x)$, and the associated weights are given as

$$\hat{w}_k = \frac{1}{(n_2+1)\hat{\mathcal{L}}_{n_2}^2(\hat{x}_k)}, \quad k = 0, 1, \ldots, n_2.$$

We define the stable Gauss–Radau–Laguerre basis function as

$$\hat{\phi}_k(x) = -\frac{\hat{\mathcal{L}}_{n_2+1}(x) - \hat{\mathcal{L}}_{n_2}(x)}{(x-\hat{x}_k)\hat{\mathcal{L}}_{n_2}(\hat{x}_k)}, \quad k = 0, 1, \ldots, n_2.$$

Note that the subscripts 1 and 2 are the parameters representing the first and second sub-domain, respectively. Furthermore, these polynomials must be continuous at the internal endpoints to enforce the continuity of the solution at the internal element boundaries.

For the European put option where the first derivative of the payoff function is discontinuous at the strike price, the interval is partitioned at K such that only two elements are sufficient to achieve high accuracy. Therefore, the infinite domain Ω will be decomposed into two sub-domains so that we let $\Omega_1 = [0, K]$ and $\Omega_2 = [K, \infty)$. For the first element, we approximate $v_1(S,\tau) = v(S,\tau)_{|S\in\Omega_1}$ using the Gauss–Lobatto–Legendre quadrature and in the second element, $v_2(S,\tau) = v(S,\tau)_{|S\in\Omega_2}$ will be expanded using the stable Gauss–Radau–Laguerre method. In the latter case, we have the following global approximation space:

$$\mathbb{X}_N = \{v \in C^0(\Omega); v_1 \in \mathbb{P}_{n_1,1}(\Omega_1),\ v_2 \in \hat{\mathbb{P}}_{n_2}(\Omega_2)\}, \quad \mathcal{X}_N = \mathbb{X}_N \cap H^1(\Omega),$$

where N is the dimension of $\mathbb{X}_N$.

4.1. Approximation results In this section, we give some approximation results related to the spectral element method. Let $\omega_\alpha(x) = x^\alpha e^{-x}$, $\hat{\omega}_\alpha(x) = x^\alpha$ and $\hat{\partial}_x = \partial_x + 1/2$. We define the space

$$\hat{B}^m(\mathbb{R}^+) = \{u \mid \hat{\partial}_x^k u \in L^2_{\hat{\omega}_k}(\mathbb{R}^+),\ 0 \le k \le m\},$$

equipped with the norm

$$\|u\|_{\hat{B}^m(\mathbb{R}^+)} = \left(\sum_{k=0}^{m} \|\hat{\partial}_x^k u\|^2_{L^2_{\hat{\omega}_k}(\mathbb{R}^+)}\right)^{1/2},$$

where $\partial_x^k u(x) = d^k u(x)/dx^k$. Some projection operators are introduced next.

Let $\Pi_{n_1}^{(1,e)} : L^2(\Omega_1^e) \to \mathbb{P}_{n_1}(\Omega_1^e)$ be the $L^2(\Omega_1^e)$-orthogonal projection operator defined by

$$(u - \Pi_{n_1}^{(1,e)} u, \phi)_{\Omega_1^e} = 0 \quad \text{for all } \phi \in \mathbb{P}_{n_1}(\Omega_1^e),$$

given $u \in L^2(\Omega_1^e)$ and let $\Pi_{n_2}^{(2)} : L^2_\omega(\Omega_2) \to \mathbb{P}_{n_2}(\Omega_2)$ be the L^2_ω-orthogonal projection operator defined by

$$(u - \Pi_{n_2}^{(2)} u, \phi)_{\omega,\Omega_2} = 0 \quad \text{for all } \phi \in \mathbb{P}_{n_2}(\Omega_2),$$

https://doi.org/10.1017/S1446181121000286 Published online by Cambridge University Press

given $u \in L^2_{\omega}(\Omega_2)$. We can then define the operator $\hat{\Pi}^2_{n_2} : L^2_{\hat{\omega}}(\Omega_2) \to \hat{\mathbb{P}}_{n_2}(\Omega_2)$ as

$$\hat{\Pi}^{(2)}_{n_2} u(x) = e^{-x/2} \Pi^{(2)}_{n_2}(u(x)e^{x/2}) \quad \text{for all } u \in L^2_{\hat{\omega}}(\Omega_2).$$

Then for any $\hat{\phi} \in \hat{\mathbb{P}}_{n_2}(\Omega_2)$,

$$(u - \hat{\Pi}^{(2)}_{n_2} u, \hat{\phi})_{\hat{\omega},\Omega_2} = (u(x)e^{x/2} - \Pi^{(2)}_{n_2}(u(x)e^{x/2}), \hat{\phi}e^{x/2})_{\omega,\Omega_2} = 0.$$

Hence, $\hat{\Pi}^{(2)}_{n_2}$ is the orthogonal projection operator from $L^2_{\hat{\omega}}(\Omega_2)$ into $\hat{\mathbb{P}}_{n_2}(\Omega_2)$.

We now define the projectors with respect to the global domain Ω. Let $\Pi_N : L^2(\Omega) \to \mathbb{X}_N$ be the orthogonal projector, defined by

$$(u - \Pi_N u, \phi_N)_{\Omega} = 0 \quad \text{for all } \phi_N \in \mathbb{X}_N,$$

given $u \in L^2(\Omega)$. Finally, let $\Pi^1_N : H^1(\Omega) \to \mathcal{X}_N$ be the $H^1(\Omega)$-orthogonal projection operator, defined by,

$$(\partial_x(u - \Pi^1_N u), \partial_x \phi_N)_{\Omega} = 0 \quad \text{for all } \phi_N \in \mathcal{X}_N,$$

given $u \in H^1(\Omega)$.

Next, we present some approximation results for the multi-domain Legendre interpolation and the modified Laguerre interpolation [26, 30]. The following results hold from the work of Quarteroni [26].

LEMMA 4.1. *Let $r \geq 1$. Then there exists a positive constant c_1 dependent only on r such that for all $u \in H^r(\Omega^e_1)$, we have*

$$\|u - \Pi^{(1,e)}_{n_1} u\|_{H^1(\Omega^e_1)} \leq c_1 h_e^{\min(n_1, r-1)} n_1^{1-r} \|u\|_{H^r(\Omega^e_1)}.$$

However, if u is continuous and composed of E pieces that are smooth in the closure of each interval Ω^e_1, $e = 1, 2, \ldots, E$, then the approximate solution will converge faster than any algebraic power, that is, the order of convergence becomes exponential. We then have an estimate of the form

$$\|u - \Pi^{(1,e)}_{n_1} u\|_{H^1(\Omega^e_1)} \leq c_1 \exp(-\gamma_e n_1). \tag{4.1}$$

Over the whole interval Ω_1, we can rewrite (4.1) such that

$$\|u - \Pi^{(1)}_{n_1} u\|_{H^1(\Omega_1)} \leq C \sum_{e=1}^{E} \exp(-\gamma_e n_1),$$

where γ_e depends on the regions Ω^1_e.

The following lemma can be found in the work of Shen et al. [30].

LEMMA 4.2. *If $u \in H^1(\Omega_2)$ and $\hat{\partial}_x u \in \hat{B}^{s-1}(\Omega_2)$, then*

$$\|u - \hat{\Pi}^{(2)}_{n_2} u\|_{H^1(\Omega_2)} \leq c_2 n_2^{(1-s)/2} \|u\|_{\hat{B}^s(\Omega_2)} \quad \text{for } 1 \leq s \leq n_2 + 1.$$

https://doi.org/10.1017/S1446181121000286 Published online by Cambridge University Press

In the same way, if u is smooth enough over Ω_2, then the error will decay exponentially fast such that

$$\|u - \hat{\Pi}^{(2)}_{n_2} u\|_{H^1(\Omega_2)} \leq c_2 \exp(-\beta n_2),$$

where β depends on the region Ω_2.

The conditions on the exponential convergence rates are determined case by case, as discussed in the work of Shen et al. [30].

4.2. Weak formulation A weak formulation of (2.1) is to find $v(\tau) \in H^1(\Omega)$ such that

$$(\mathcal{D}^{\alpha}_{\tau} v(\tau), \varphi)_{\Omega} + \mathcal{A}_{\Omega}(v(\tau), \varphi) = b(\tau) \quad \text{for all } \varphi \in H^1(\Omega), \tag{4.2}$$

where $(\mathcal{D}^{\alpha}_{\tau} v(\tau), \varphi)_{\Omega} = \int_{\Omega} \mathcal{D}^{\alpha}_{\tau} v(S, \tau)\varphi(S)\, dS$. Note that here,

$$A_{\Omega}(v(\tau), \varphi) = \frac{1}{2}\sigma^2 \int_{\Omega} S^2 \frac{\partial v(S,\tau)}{\partial S}\frac{\partial \varphi}{\partial S}\, dS - (r - \delta - \sigma^2) \int_{\Omega} S \frac{\partial v(S,\tau)}{\partial S}\varphi(S)\, dS + r \int_{\Omega} v(S,\tau)\varphi(S)\, dS,$$

where $\varphi \in H^1(\Omega)$ is a trial function that satisfies certain boundary conditions and

$$b(\tau) = \frac{1}{2}\sigma^2 \left[S^2 \frac{\partial v(S,\tau)}{\partial S}\varphi(S) \right]_0^{\infty}.$$

The approximation of (4.2) by the spectral element method can be obtained by finding $\hat{v}(\tau) \in \mathcal{X}_N$ such that

$$(\mathcal{D}^{\alpha}_{\tau} \hat{v}(\tau), \varphi)_{\Omega} + \mathcal{A}_{\Omega}(\hat{v}(\tau), \varphi) = b(\tau) \quad \text{for all } \varphi \in \mathcal{X}_N. \tag{4.3}$$

Equivalently, (4.3) can be rewritten as: find $\hat{v}(\tau)$ such that

$$(\mathcal{D}^{\alpha}_{\tau} \hat{v}(\tau), \varphi)_{\Omega_1} + (\mathcal{D}^{\alpha}_{\tau} \hat{v}(\tau), \varphi)_{\Omega_2} + \mathcal{A}_{\Omega_1}(\hat{v}(\tau), \varphi) + \mathcal{A}_{\Omega_2}(\hat{v}(\tau), \varphi) = b(\tau) \quad \text{for all } \varphi \in \mathcal{X}_N,$$

upon Ω_1 and Ω_2. Before applying the Gauss–Lobatto–Legendre and Gauss–Radau–Laguerre methods, we must first transform the sub-domains to corresponding reference domains as follows:

$$S = \mathrm{J}^{(1)}(x + 1), \quad \mathrm{J}^{(1)} = \frac{K}{2}, \quad x \in [-1, 1], \quad S \in \Omega_1,$$
$$S = \mathrm{J}^{(2)}\hat{x} + K, \quad \mathrm{J}^{(2)} = \frac{S_{\max} - K}{\hat{x}_{n_2}}, \quad \hat{x} \in [0, \infty), \quad S \in \Omega_2,$$

where $\mathrm{J}^{(1)}$ and $\mathrm{J}^{(2)}$ are the Jacobians of the transformations of Ω_1 and Ω_2, respectively, and $\hat{x}_{n_2}$ is the last grid point for the stable Gauss–Radau–Laguerre basis function.

For the option price to be continuous at the strike price, the last grid point of the first element and the first grid point of the second element will be taken as one

https://doi.org/10.1017/S1446181121000286 Published online by Cambridge University Press

single point, that is, $S_{n_1}^{(1)} = S_0^{(2)}$ such that we have $N = n_1 + n_2 + 1$ distinct points. These approximations also require that $\phi_{n_1} = \hat{\phi}_0$. The approximate solution over the whole domain can then be represented as

$$\hat{v}(S,\tau) = \sum_{l=0}^{n_1} \hat{v}_1(S_l,\tau)\phi_l(S)\Big|_{S\in\Omega_1} + \sum_{l=1}^{n_2} \hat{v}_2(S_l,\tau)\hat{\phi}_l(S)\Big|_{S\in\Omega_2}.$$

However, the weak formulation has to be considered separately for each element. The option price will then be obtained after the proper assemblage according to the structure of the global basis function. Taking $\varphi = \phi_m$ in the first element and $\varphi = \hat{\phi}_m$ for the second element, we have, after the transformations in each element,

$$\begin{aligned}(\mathcal{D}_\tau^\alpha \hat{v}(\tau),\varphi)_{\Omega_1} + \mathcal{A}_{\Omega_1}(\hat{v}(\tau),\varphi) = \mathrm{J}^{(1)} &\sum_{l=0}^{n_1} \mathcal{D}_\tau^\alpha \hat{v}_1(S_l,\tau) \int_{-1}^{1} \phi_l(x)\phi_m(x)\,dx \\ &+ \frac{1}{2\mathrm{J}^{(1)}}\sigma^2 \sum_{l=0}^{n_1} \hat{v}_1(S_l,\tau) \int_{-1}^{1} S^2 \frac{\partial\phi_l(x)}{\partial x}\frac{\partial\phi_m(x)}{\partial x}\,dx \\ &- (r-\delta-\sigma^2) \sum_{l=0}^{n_1} \hat{v}_1(S_l,\tau) \int_{-1}^{1} S\frac{\partial\phi_l(x)}{\partial x}\phi_m(x)\,dx \\ &+ r\mathrm{J}^{(1)} \sum_{l=0}^{n_1} \hat{v}_1(S_l,\tau) \int_{-1}^{1} \phi_l(x)\phi_m(x)\,dx, \end{aligned} \tag{4.4}$$

over the first element for $m = 0, 1, \ldots, n_1$ and $S \in \Omega_1$, and

$$\begin{aligned}(\mathcal{D}_\tau^\alpha \hat{v}(\tau),\varphi)_{\Omega_2} + \mathcal{A}_{\Omega_2}(\hat{v}(\tau),\varphi) = \mathrm{J}^{(2)} &\sum_{l=0}^{n_2} \mathcal{D}_\tau^\alpha \hat{v}_2(S_l,\tau) \int_{0}^{\infty} \hat{\phi}_l(x)\hat{\phi}_m(x)\,dx \\ &+ \frac{1}{2\mathrm{J}^{(2)}}\sigma^2 \sum_{l=0}^{n_2} \hat{v}_2(S_l,\tau) \int_{0}^{\infty} S^2 \frac{\partial\hat{\phi}_l(x)}{\partial x}\frac{\partial\hat{\phi}_m(x)}{\partial x}\,dx \\ &- (r-\delta-\sigma^2) \sum_{l=0}^{n_2} \hat{v}_2(S_l,\tau) \int_{0}^{\infty} S\frac{\partial\hat{\phi}_l(x)}{\partial x}\hat{\phi}_m(x)\,dx \\ &+ r\mathrm{J}^{(2)} \sum_{l=0}^{n_2} \hat{v}_2(S_l,\tau) \int_{0}^{\infty} \hat{\phi}_l(x)\hat{\phi}_m(x)\,dx, \end{aligned} \tag{4.5}$$

in the second element for $m = 0, 1, \ldots, n_2$ and $S \in \Omega_2$. Note that the boundary term $b(\tau)$ vanishes naturally when $S = 0$ and since $\varphi(S) = \hat{\phi}(x)$ in the second element decays exponentially with S, $b(\tau)$ also vanishes as $S \to \infty$.

https://doi.org/10.1017/S1446181121000286 Published online by Cambridge University Press

In general, the integration terms, which we call the mass, advection and stiffness matrices, can be written as

$$M_{lm}^{(e)} = \mathrm{J}\int \psi_l(\xi)\psi_m(\xi)\,d\xi = \mathrm{J}^{(e)}\sum_{k=0}^{n}\gamma_k\psi_l(\xi_k)\psi_m(\xi_k) = \mathrm{J}^{(e)}\gamma_l\delta_{lm},$$

$$A_{lm}^{(e)} = \int S(\xi)\frac{\partial\psi_l(\xi)}{\partial\xi}\psi_m(\xi)\,d\xi = \sum_{k=0}^{n}\gamma_k S(\xi_k)D_{kl}\delta_{km} = \gamma_m S(\xi_m)D_{ml},$$

$$\mathcal{S}_{lm}^{(e)} = \frac{1}{\mathrm{J}^{(e)}}\int S(\xi)^2\frac{\partial\psi_l(\xi)}{\partial\xi}\frac{\partial\psi_m(\xi)}{\partial\xi}\,d\xi = \frac{1}{\mathrm{J}^{(e)}}\sum_{k=0}^{n}\gamma_k S(\xi_k)^2 D_{kl}D_{km},$$

respectively, where ψ, γ and D represent the basis function, weights and first-derivative matrix of the basis function of the associated Gauss quadrature, respectively. In matrix form, we can then write

$$\mathbf{M}^{(e)} = \mathrm{J}^{(e)}\mathbf{W}^{(e)}, \quad \mathbf{A}^{(e)} = \mathbf{S}^{(e)}\mathbf{W}^{(e)}\mathbf{D}^{(e)} \quad \text{and} \quad \boldsymbol{\mathcal{S}}^{(e)} = \frac{1}{\mathrm{J}^{(e)}}\mathbf{D}^{(e)^\top}(\mathbf{S}^{(e)})^2\mathbf{W}^{(e)}\mathbf{D}^{(e)},$$

where $\mathbf{W}^{(e)}$ and $\mathbf{S}^{(e)}$ are the diagonal matrices of the associated quadrature weights and element-wise asset price values, respectively. Each local matrix will then be assembled to form global matrices $\mathbf{M}$, $\mathbf{A}$ and $\boldsymbol{\mathcal{S}}$. This assembly procedure couples the contribution of each element together [36].

Let $\bar{v}(\tau) = [\hat{v}_1(S_0,\tau), \hat{v}_1(S_1,\tau), \ldots, \hat{v}_1(S_{n_1},\tau), \hat{v}_2(S_1,\tau), \hat{v}_2(S_2,\tau), \ldots, \hat{v}_2(S_{n_2},\tau)]^\top$ be the vector of the European put option prices, then the generated semi-discrete system is of the form

$$\mathbf{M}(\mathcal{F}_\tau^\alpha\bar{v}(\tau)) = \mathbf{L}\bar{v}(\tau), \tag{4.6}$$

where $\mathbf{L} = -(\sigma^2/2)\boldsymbol{\mathcal{S}} + (r-\delta-\sigma^2)\mathbf{A} - r\mathbf{M}$ is the matrix system obtained after the assembly of each local matrix from (4.4) and (4.5). Based on the $L1$ approximation (3.3) of the time-fractional derivative, (4.6) then becomes

$$(\mathbf{M} - \alpha_0\mathbf{L})\bar{v}^{m+1} = \mathbf{M}\sum_{j=0}^{m-1}(b_j - b_{j+1})\bar{v}^{m-j} + b_m\mathbf{M}\bar{v}^0, \tag{4.7}$$

for $m = 0, 1, \ldots, M-1$.

For the double knock-out call barrier option, we have Dirichlet boundary conditions and one more discontinuity exists at the upper barrier level in its payoff such that we use three elements: $\Omega_1 = [B_l, K]$, $\Omega_2 = [K, B_u]$ and $\Omega_3 = [B_u, \infty)$. In this case, we approximate $v_1(S,\tau) = v(S,\tau)_{|S\in\Omega_1}$ and $v_2(S,\tau) = v(S,\tau)_{|S\in\Omega_2}$ using the Gauss–Lobatto–Legendre quadrature and $v_3(S,\tau) = v(S,\tau)_{|S\in\Omega_3}$ is expanded using the stable Gauss–Radau–Laguerre method such that the approximate solution over Ω can

https://doi.org/10.1017/S1446181121000286 Published online by Cambridge University Press

be represented as

$$\hat{v}(S,\tau) = \sum_{l=0}^{n_1} \hat{v}_1(S_l,\tau)\phi_l(S)\Big|_{S\in\Omega_1} + \sum_{l=1}^{n_2} \hat{v}_2(S_l,\tau)\phi_l(S)\Big|_{S\in\Omega_2} + \sum_{l=1}^{n_3} \hat{v}_3(S_l,\tau)\hat{\phi}_l(S)\Big|_{S\in\Omega_3},$$

where n_3 is, in this case, the degree of the modified Laguerre polynomials. To deal with the discontinuity at the upper barrier level, we adopt the discontinuous payoff spectral element method as in the work of Yue [36]. The left and right parts of the payoff function shall be considered separately at the initial time. With $v_L(0)$ and $v_R(0)$ being the barrier's initial payoff at the immediate left and right to the barrier level, B_u, then $\hat{v}(0)_{|\Omega_1,\Omega_2} = v_L(0) = S - K$ and $\hat{v}(0)_{|\Omega_3} = v_R(0) = 0$. Over a tiny time step $\Delta\tau = 10^{-11}$ after the initial time, we use the Crank–Nicolson scheme [11] such that

$$[\mathbf{M} - \tfrac{1}{2}\Delta\tau\mathbf{L}]\bar{v}(\tau_m) = [\mathbf{M}_L + \tfrac{1}{2}\Delta\tau\mathbf{L}_L]\bar{v}_L(0) + [\mathbf{M}_R + \tfrac{1}{2}\Delta\tau\mathbf{L}_R]\bar{v}_R(0),$$

where $\mathbf{M}_L$, $\mathbf{L}_L$, $\mathbf{M}_R$, $\mathbf{L}_R$ are the left and right global matrices. More details about the structures of these matrices can be found in the work of Yue [36]. Then for the remaining time, $T - \Delta\tau$, the same procedure as for the European option can be implemented to obtain the option price.

5. Richardson extrapolation

To improve the accuracy in time, we consider the Richardson extrapolation process with s stages [15] which is described next. As shown in several works [13, 24, 35], the approximated solutions of fractional order differential equations possess asymptotic expansions with respect to the step size. In the same way, to apply the Richardson extrapolation approach in time to guarantee higher order convergence, we assume the existence of asymptotic expansions for solutions obtained using the $L1$ scheme to approximate the Caputo time fractional derivative [22]. We emphasize that the $L1$ approximation scheme will only be $O((\Delta\tau)^{2-\alpha})$ provided the considered function is twice continuously differentiable. However, for the European and barrier options, $v(S,\tau)$ is only once continuously differentiable with respect to time such that only first-order accuracy can be attained [18]. A sequence of approximations to $v(\Delta\tau)$ can be constructed using the discretization method (4.7). Let $v_{k,l}$ denote the approximate solution obtained using the $L1$ scheme at time $\Delta\tau$ with step size $\Delta\tau/2^{k-1}$, $k = 1, 2, \ldots, s$. As such, with prior knowledge of the rate of convergence of the $L1$ discretization, we have the following s-stage extrapolation tableau given by

$$\hat{v}_{k,l} = \frac{(2)^{k-1}\hat{v}_{k,l-1} - \hat{v}_{k-1,l-1}}{(2)^{k-1} - 1}, \tag{5.1}$$

for $k = 2, \ldots, s$ and $l = 2, \ldots, k$. Starting with M initial time steps and doubling M at each extrapolation stage, the total number of time steps required after using the s-stage Richardson extrapolation is $M_s = (2^s - 1)M$.

https://doi.org/10.1017/S1446181121000286 Published online by Cambridge University Press

We next provide the algorithm for finding the European option value.

Algorithm 1: Legendre–Laguerre spectral approximation [26, 30] and the Richardson extrapolation approach for pricing European options under the time fractional Black–Scholes model.

- Initialise all problem parameters.
- Calculate the nodes and weights $\{x_k, w_k\}$ and $\{\hat{x}_k, \hat{w}_k\}$ for the Gauss-Lobatto-Legendre and stable Gauss-Radau-Laguerre methods.
- Transform the spatial sub-domains to corresponding reference domains.
- Construct the mass, advection and stiffness matrices $\mathbf{M}^{(e)}$, $\mathbf{A}^{(e)}$ and $\boldsymbol{\mathcal{S}}^{(e)}$ respectively.
- Assemble each local matrix according to the number of elements to form global matrices $\mathbf{M}$, $\mathbf{A}$ and $\boldsymbol{\mathcal{S}}$.
- Calculate the weights b_j for the L_1 approximation.

for *each extrapolation stage* **do**
  Calculate $dt = T/M$.
  for *m = 1 to M* **do**
    Solve (4.7).
  end
  Double M
end

- Use (5.1) to find the extrapolated solution.

6. Numerical results

This section presents the numerical results to illustrate the efficiency of the Legendre–Laguerre spectral approximation and the Richardson extrapolation approach to price the European put and double barrier call options governed by the time-fractional Black–Scholes equation. All computations of our numerical experiments have been performed using MATLAB® with a Core i5, 2.50 GHz processor and 8 GB RAM. With no analytical solutions available for option prices in the fractional framework, we consider reference solutions calculated over more refined grids with $n_1 = n_2 = 40$ in the spatial direction and $s = 6$ starting with an initial $M = 20$ in the temporal direction. The errors are given in the L^2, L^∞ and H^1 norms such that Error $= v_{\text{ref}} - v_N^M$, where v_{ref} is a vector of reference prices and V_N^M represents the corresponding approximate computed solutions. The rates of convergence in the temporal direction can be computed by

$$\text{Rate}_{\Delta\tau} = \log_2\left(\frac{\|\text{Error}(\Delta\tau)\|}{\|\text{Error}(\Delta\tau/2)\|}\right).$$

For the first numerical experiment, we consider the same first example as in the work of Zhang et al. [38].

https://doi.org/10.1017/S1446181121000286 Published online by Cambridge University Press

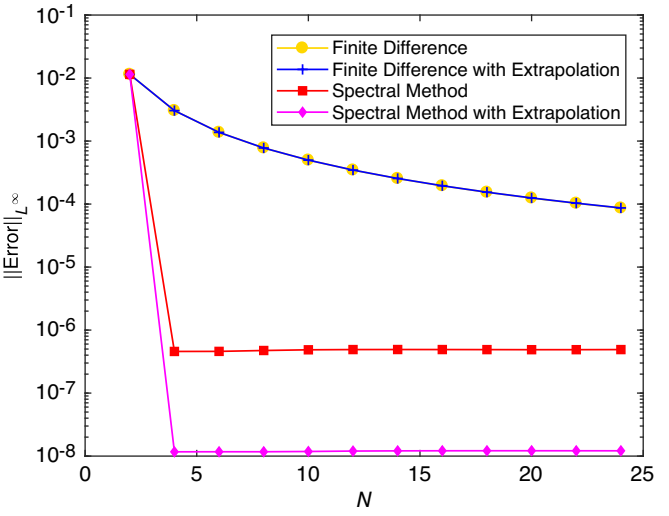

FIGURE 1. Log plot of maximum errors against N for Example 6.1 for the finite-difference and spectral methods with $\alpha = 0.7$.

EXAMPLE 6.1. Consider the following time-fractional equation with homogeneous boundary conditions:

$$\mathcal{D}_\tau^\alpha u(x,\tau) = a\frac{\partial^2 u(x,\tau)}{\partial x^2} + b\frac{\partial u(x,\tau)}{\partial x} - cu(x,\tau) + g(x,\tau), \quad x \in (0,1),\ \tau \in (0,T],$$

where

$$g(x,\tau) = \left[\frac{2\tau^{2-\alpha}}{\Gamma(3-\alpha)} + \frac{2\tau^{1-\alpha}}{\Gamma(2-\alpha)}\right]x^2(1-x) - (\tau+1)^2[a(2-6x) + b(2x-3x^2) - cx^2(1-x)].$$

The initial and boundary conditions are

$$u(x,0) = x^2(1-x),$$
$$u(0,\tau) = 0 \ \text{ and } \ u(1,\tau) = 0.$$

The exact analytical solution to this problem is $u(x,\tau) = (\tau+1)^2x^2(1-x)$.

Here the parameters are chosen as in the work of Zhang et al. [38], that is,

$$r = 0.05, \quad \sigma = 0.25, \quad T = 1, \quad a = \tfrac{1}{2}\sigma^2, \quad b = r - a, \quad c = r.$$

In Figure 1, we compare the second-order finite-difference scheme used in the work of Zhang et al. [38] to the spectral approximation using only Legendre basis functions for Example 6.1 with the $L1$ approximation approach for the time discretization. Figure 1 also illustrates the performance of the extrapolation approach when used with both the finite-difference scheme and the spectral element discretization. We plot here the

https://doi.org/10.1017/S1446181121000286 Published online by Cambridge University Press

TABLE 1. The L^2 and H^1 errors for the $L1$ approximation and the Richardson extrapolation approach for Example 6.1.

$L1$ approximation					Extrapolation				
M	$\|\|\text{Error}\|\|_{L^2}$	$\text{Rate}_{\Delta\tau}$	$\|\|\text{Error}\|\|_{H^1}$	$\text{Rate}_{\Delta\tau}$	s	$\|\|\text{Error}\|\|_{L^2}$	$\text{Rate}_{\Delta\tau}$	$\|\|\text{Error}\|\|_{H^1}$	$\text{Rate}_{\Delta\tau}$
$\alpha = 0.5$									
20	5.5e −4	–	1.9e −3	–	1	–	–	–	–
40	2.0e −4	1.4676	6.9e −4	1.4682	2	6.8e −6	–	2.3e −5	–
80	7.1e −5	1.4782	2.5e −4	1.4786	3	9.1e −7	2.9016	3.1e −6	2.8913
160	2.5e −5	1.4851	8.8e −5	1.4854	4	1.9e −7	2.2599	6.6e −7	2.1844
320	9.0e −6	1.4897	3.1e −5	1.4899	5	4.6e −8	2.0463	1.6e −7	2.0444
$\alpha = 0.7$									
20	1.5e −3	–	5.1e −3	–	1	–	–	–	–
40	6.1e −4	1.2808	2.1e −3	1.2814	2	1.4e −5	–	4.6e −5	–
80	2.5e −4	1.2889	8.6e −4	1.2892	3	1.2e −6	3.5443	4.0e −6	3.5236
160	1.0e −4	1.2935	3.5e −4	1.2937	4	2.2e −7	2.4475	7.5e −7	2.4150
320	4.1e −5	1.2961	1.4e −4	1.2963	5	5.0e −8	2.1375	4.9e −8	3.9360
$\alpha = 0.9$									
20	3.6e −3	–	1.3e −2	–	1	–	–	–	–
40	1.7e −3	1.0891	6.0e −3	1.0890	2	2.4e −5	–	8.5e −5	–
80	8.0e −4	1.0942	2.8e −3	1.0941	3	1.1e −6	4.4475	3.5e −6	4.6020
160	3.7e −4	1.0969	1.3e −3	1.0969	4	1.6e −7	2.7814	5.3e −7	2.7233
320	1.7e −4	1.0983	6.1e −4	1.0984	5	3.3e −8	2.2775	1.1e −7	2.2685

errors in the L^∞ norm against N, the total number of grid nodes for the finite-difference and spectral methods. To eliminate the temporal error, we fix $M = 10\,000$ for the $L1$ scheme and we use $s = 6$ starting with an initial $M = 20$ using the extrapolation approach. From Figure 1, we can observe the superior performance of the spectral method over the finite-difference approach, where the maximum errors for the spectral approximation decrease much faster than the finite-difference method which converges algebraically. Note that $N = 5$ is sufficient to achieve 10^{-6} accuracy for the spectral method, while many more grid nodes will be required to reach the same level of accuracy using the finite-difference approach. Applying the extrapolation process, we can see the faster convergence of the spectral method while the extrapolated solution with the finite-difference scheme behaves in a similar way as the nonextrapolated scheme, since not enough grid nodes are used to achieve the required accuracy. We point out that similar graphs are obtained in the L^2 and H^1 norms.

In Table 1, we report the L^2 and H^1 errors for the time-fractional model in Example 6.1 using the $L1$ approximation and the Richardson extrapolation approach for

https://doi.org/10.1017/S1446181121000286 Published online by Cambridge University Press

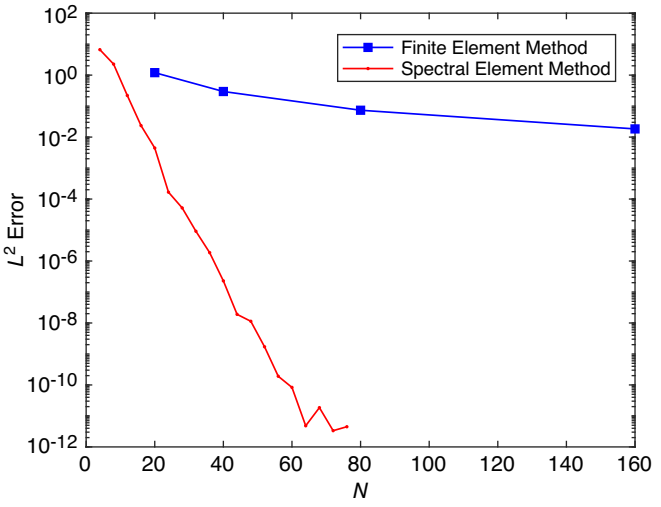

FIGURE 2. Log plot of L^2 errors against N for a European put option with $\alpha = 0.9$ with the finite element and spectral element methods.

$\alpha = 0.5$, 0.7 and 0.9. It can be observed that the convergence rates for the $L1$ method are indeed $O((\Delta\tau)^{2-\alpha})$ for the different values of α. Based on these rates of convergence, we can see the faster convergence of the Richardson extrapolation approach for all the values of α considered. Note that many more time steps would be required to reach the same level of accuracy without extrapolation.

6.1. European options We now consider the numerical comparison for the space discretization for the European put option under the time-fractional Black–Scholes model with parameters chosen as

$$K = 50,\ r = 0.05,\ \sigma = 0.25,\ \delta = 0,\ T = 1.$$

In Figure 2, we compare the spectral element method with the finite element discretization under the time-fractional Black–Scholes framework, where the errors for the European put option are presented in the L^2 norms against the total number of grid nodes, N, to check the spatial accuracy for $\alpha = 0.9$. We can clearly see that the errors decay exponentially with far fewer mesh points which shows spectral accuracy compared with the linear finite element method achieving only second-order convergence. This validates that the theoretical results in Lemma 4.1 and Lemma 4.2 for the European option have adequate smooth solutions in the closure of each interval Ω_1 and Ω_2.

Using the $L1$ scheme, we observe from Table 2 that only first-order convergence in time is achieved for $\alpha = 0.1, 0.3$ and 0.7. Higher accuracy is obtained using the Richardson extrapolation approach in much fewer time steps. Obviously, European

https://doi.org/10.1017/S1446181121000286 Published online by Cambridge University Press

TABLE 2. The L^2 and L^∞ errors for the European option for the $L1$ approximation and the Richardson extrapolation approach.

$L1$ approximation					Extrapolation				
M	$\|\|\text{Error}\|\|_{L^2}$	$\text{Rate}_{\Delta\tau}$	$\|\|\text{Error}\|\|_{L^\infty}$	$\text{Rate}_{\Delta\tau}$	s	$\|\|\text{Error}\|\|_{L^2}$	$\text{Rate}_{\Delta\tau}$	$\|\|\text{Error}\|\|_{L^\infty}$	$\text{Rate}_{\Delta\tau}$
$\alpha = 0.1$									
20	3.5e −2	–	6.1e −3	–	1	–	–	–	–
40	1.7e −2	1.0163	3.0e −3	1.0163	2	3.9e −4	–	6.8e −5	–
80	8.6e −2	1.0085	1.5e −3	1.0086	3	5.1e −6	6.2568	9.5e −7	6.1615
160	4.3e −2	1.0045	7.4e −4	1.0045	4	1.3e −6	1.9720	2.3e −7	2.0463
320	2.1e −2	1.0024	3.7e −4	1.0024	5	2.2e −7	2.5629	4.0e −8	2.5236
$\alpha = 0.3$									
20	1.1e −1	–	2.0e −2	–	1	–	–	–	–
40	5.6e −2	1.0221	9.7e −3	1.0195	2	1.6e −3	–	2.7e −4	–
80	2.8e −2	1.0126	4.8e −3	1.0117	3	1.0e −4	4.0000	1.7e −5	3.9894
160	1.4e −2	1.0076	2.4e −3	1.0071	4	2.2e −5	2.1844	3.6e −6	2.2395
320	6.9e −3	1.0045	1.2e −3	1.0042	5	4.4e −6	2.3219	7.4e −7	2.2824
$\alpha = 0.7$									
20	2.4e −1	–	3.9e −2	–	1	–	–	–	–
40	1.2e −1	0.9743	2.0e −2	0.9602	2	6.2e −3	–	1.2e −3	–
80	6.3e −2	0.9806	1.0e −2	0.9695	3	1.1e −3	2.4948	2.1e −4	2.5146
160	3.2e −2	0.9852	5.2e −3	0.9763	4	3.3e −4	1.7370	6.3e −5	1.7370
320	1.6e −2	0.9892	2.6e −3	0.9825	5	8.5e −5	1.9569	1.7e −5	1.8898

option prices can be calculated more accurately than with the $L1$ scheme for different values of α as done so far in the literature.

We further illustrate the computational efficiency of the extrapolation approach in Figure 3. In particular, we plot the L^2 errors against M and computational times in seconds in log–log scale in Figures 3(a) and 3(b), respectively. We observe the faster convergence of the extrapolation scheme where a total of 620 time steps are needed to achieve an accuracy of 10^{-5} in contrast to $M = 327\,680$ for the $L1$ method to reach the same accuracy. We further observe that the computational times for the $L1$ scheme are much higher than for the extrapolation method where the accuracy of 10^{-5} is achieved in 0.1052 seconds with the extrapolation approach compared with 43 090 seconds for the commonly used $L1$ scheme. It is obvious that a simple extrapolation approach is very efficient to achieve high accuracy with much fewer time steps. The practical importance of the present contribution therefore stems from the fact that the computational requirement for storing the numerical solution for all previous time steps is much less for an extrapolation scheme compared with a first-order scheme to reach similar levels of accuracy.

https://doi.org/10.1017/S1446181121000286 Published online by Cambridge University Press

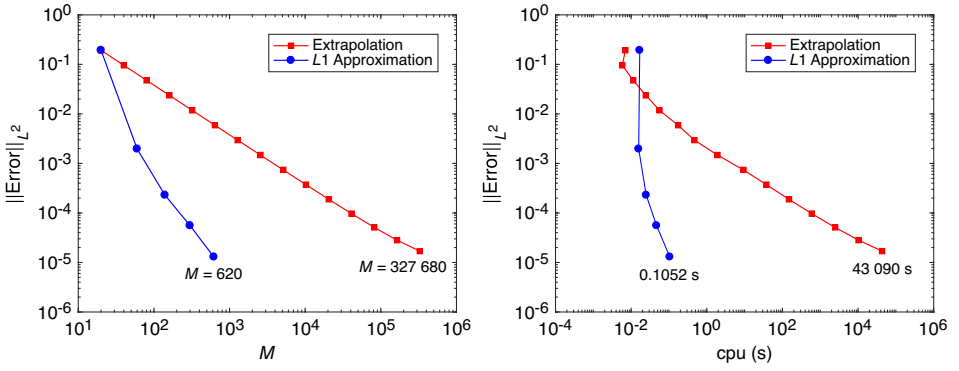

(a) L^2 errors. (b) Computational times in seconds.

FIGURE 3. Log–log plots of L^2 errors and computational times in seconds for the $L1$ scheme and the Richardson extrapolation method for a European put option under the time-fractional Black–Scholes model for $\alpha = 0.5$.

6.2. Double barrier options For the next test problem, we consider the double knock-out call barrier option with the following model parameters:

$$K = 10, \quad r = 0.03, \quad \sigma = 0.45, \quad \delta = 0, \quad T = 1, \quad B_l = 3, \quad B_u = 15.$$

As previously mentioned, we use three elements, and only one node is sufficient for the third element to enforce the upper boundary. As such, for the error stemming from the spectral approximation to be negligible, we choose $n_1 = n_2 = 40$ and $n_3 = 1$. Table 3 reports the errors in the L^2 norm for $\alpha = 0.1, 0.3, 0.5, 0.7$ for the $L1$ approximation and the Richardson extrapolation approach for the double barrier call option. Again first-order accuracy is obtained using the $L1$ method while the Richardson extrapolation approach gives higher accuracy.

7. Conclusion

In this work, under the time-fractional Black–Scholes model, we considered a Legendre–Laguerre spectral approximation to price European and double barrier options. By breaking the domain into sub-domains, the option price within each element is approximated by the Legendre and Laguerre basis functions with the associated quadrature rules. A comparison with the second-order finite-difference approach indicates that the spectral approximation gives a viable alternative to the latter with far fewer grid points necessary to obtain highly accurate solutions in space. Consequently, at each time step, only linear systems of moderate dimensions are required to be solved, thus making the proposed scheme computationally faster and more efficient. To further improve the temporal convergence, a Richardson

https://doi.org/10.1017/S1446181121000286 Published online by Cambridge University Press

TABLE 3. The L^2 errors for the $L1$ approximation and the Richardson extrapolation approach for the double knock-out call barrier option.

$L1$ Approximation				Extrapolation		$L1$ Approximation				Extrapolation	
$\alpha = 0.1$						$\alpha = 0.3$					
M	$\|\|\text{Error}\|\|_{L^2}$	Rate $_{\Delta\tau}$	s	$\|\|\text{Error}\|\|_{L^2}$	Rate $_{\Delta\tau}$	M	$\|\|\text{Error}\|\|_{L^2}$	Rate $_{\Delta\tau}$	s	$\|\|\text{Error}\|\|_{L^2}$	Rate $_{\Delta\tau}$
20	4.0e −4	–	1	1	–	20	1.3e −3	–	1	–	–
40	2.0e −4	1.0159	2	4.3e −6	–	40	6.3e −4	1.0284	2	2.5e −5	–
80	9.7e −5	1.0082	3	3.0e −8	7.1632	80	3.1e −4	1.0164	3	1.2e −6	4.3808
160	4.9e −5	1.0043	4	9.8e −9	1.6141	160	1.5e −4	1.0096	4	2.7e −7	2.1520
320	2.4e −5	1.0022	5	1.7e −9	2.5272	320	7.6e −5	1.0056	5	5.5e −8	2.2955
$\alpha = 0.5$						$\alpha = 0.7$					
M	$\|\|\text{Error}\|\|_{L^2}$	Rate $_{\Delta\tau}$	s	$\|\|\text{Error}\|\|_{L^2}$	Rate $_{\Delta\tau}$	M	$\|\|\text{Error}\|\|_{L^2}$	Rate $_{\Delta\tau}$	s	$\|\|\text{Error}\|\|_{L^2}$	Rate $_{\Delta\tau}$
20	2.4e −3	–	1	–	–	20	4.3e −3	-	1	–	–
40	1.2e −3	1.0477	2	7.9e −5	–	40	2.1e −3	1.0626	2	1.8e −4	–
80	5.8e −4	1.0316	3	7.6e −6	3.3778	80	1.0e −3	1.0477	3	2.8e −5	2.6845
160	2.8e −4	1.0212	4	2.0e −6	1.9260	160	5.0e −4	1.0364	4	8.3e −6	1.7542
320	1.4e −4	1.0139	5	4.6e −7	2.1203	320	2.4e −4	1.0267	5	2.2e −6	1.9156

extrapolation scheme is applied based on the $L1$ approximation and, as demonstrated by the numerical results, this approach is very efficient to achieve higher accuracies in much fewer time steps.

Acknowledgements

The authors gratefully acknowledge the funding support under the award number ID-2019-14 from the Tertiary Education Commission, Mauritius. The authors would also like to thank the anonymous reviewers for their valuable suggestions which have brought important enhancements to this work in a significant way.

References

[1] F. Black and M. Scholes, "The pricing of options and other corporate liabilities", *J. Polit. Econ.* **81** (1973) 637–654, available at https://www.jstor.org/stable/1831029.

[2] Z. Cen, J. Huang, A. Xu and A. Le, "Numerical approximation of a time-fractional Black–Scholes equation", *Comput. Math. Appl.* **75** (2018) 2874–2887; doi:10.1016/j.camwa.2018.01.016.

[3] C. Chen, Z. Wang and Y. Yang, "A new operator splitting method for American options under fractional Black–Scholes models", *Comput. Math. Appl.* **77** (2019) 2130–2144; doi:10.1016/j.camwa.2018.12.007.

[4] H. Chen, S. Lü and W. Chen, "Finite difference/spectral approximations for the distributed order time fractional reaction-diffusion equation on an unbounded domain", *J. Comput. Phys.* **315** (2016) 84–97; doi:10.1016/j.jcp.2016.03.044.

[5] H. Chen, S. Lü and W. Chen, "Spectral and pseudospectral approximations for the time fractional diffusion equation on an unbounded domain", *J. Comput. Appl. Math.* **304** (2016) 43–56; doi:10.1016/j.cam.2016.03.010.

[6] W. Chen and S. Wang, "A 2nd-order ADI finite difference method for a 2D fractional Black–Scholes equation governing European two asset option pricing", *Math. Comput. Simulation* **171** (2020) 279–293; doi:10.1016/j.matcom.2019.10.016.

[7] W. Chen, X. Xu and S. Zhu, "Analytically pricing European-style options under the modified Black–Scholes equation with a spatial-fractional derivative", *Quart. Appl. Math.* **72** (2014) 597–611, available at https://www.jstor.org/stable/43639126.

[8] W. Chen, X. Xu and S. P. Zhu, "A predictor-corrector approach for pricing American options under the finite moment log-stable model", *Appl. Numer. Math.* **97** (2015) 15–29; doi:10.1016/j.apnum.2015.06.004.

[9] W. Chen, X. Xu and S. P. Zhu, "Analytically pricing double barrier options based on a time-fractional Black–Scholes equation", *Comput. Math. Appl.* **69** (2015) 1407–1419; doi:10.1016/j.camwa.2015.03.025.

[10] X. Chen, D. Ding, S-L. Lei and W. Wang, "A fast preconditioned iterative method for two-dimensional options pricing under fractional differential models", *Comput. Math. Appl.* **79** (2020) 440–456; doi:10.1016/j.camwa.2019.07.010.

[11] J. Crank and P. Nicolson, "A practical method for numerical evaluation of solutions of partial differential equations of the heat conduction type", *Math. Proc. Cambridge Philos. Soc.* **43** (1947) 50–67; doi: 10.1017/S0305004100023197.

[12] R. H. De Staelen and A. S. Hendy, "Numerically pricing double barrier options in a time-fractional Black–Scholes model". *Comput. Math. Appl.* **74** (2017) 1166–1175; doi:10.1016/j.camwa.2017.06.005.

[13] K. Diethelm and G. Walz, "Numerical solution of fractional order differential equations by extrapolation", *Numer. Algorithms* **16** (1997) 231–253; doi:10.1023/A:1019147432240.

[14] A. Farhadi, M. Salehi and G. H. Erjaee, "A new version of Black–Scholes equation presented by time-fractional derivative", *Iran J. Sci. Technol. Trans. A Sci.* **42** (2018) 2159–2166; doi:10.1007/s40995-017-0244-7.

[15] L. Feng and V. Linetsky, "Pricing options in jump-diffusion models: an extrapolation approach", *Oper. Res.* **56** (2008) 304–325, available at http://www.jstor.org/stable/25147189.

[16] A. Golbabai, O. Nikan and T. Nikazad, "Numerical analysis of time fractional Black–Scholes European option pricing model arising in financial market", *Comput. Appl. Math.* **38** (2019) 173; doi:10.1007/s40314-019-0957-7.

[17] J. Huang, Z. Cen and J. Zhao, "An adaptive moving mesh method for a time-fractional Black–Scholes equation", *Adv. Difference Equ.* **2019** (2019) 516; doi:10.1186/s13662-019-2453-1.

[18] B. Jin, R. Lazarov and Z. Zhou, "An analysis of the L1 scheme for the subdiffusion equation with nonsmooth data", *IMA J. Numer. Anal.* **36** (2016) 197–221; doi:10.1093/imanum/dru063.

[19] G. Jumarie, "Derivation and solutions of some fractional Black–Scholes equations in coarse-grained space and time. Application to Merton's optimal portfolio", *Comput. Math. Appl.* **59** (2010) 1142–1164; doi:10.1016/j.camwa.2009.05.015.

[20] M. Koleva and L. Vulkov, "Numerical solution of time-fractional Black–Scholes equation", *Comput. Appl. Math.* **36** (2017) 1699–1715; doi:10.1007/s40314-016-0330-z.

[21] Y. Lin, X. Li and C. Xu, "Finite difference/spectral approximations for the fractional cable equation", *Math. Comp.* **80** (2011) 1369–1396; doi:10.1090/S0025-5718-2010-02438-X.

[22] Y. Lin and C. Xu, "Finite difference/spectral approximations for the time-fractional diffusion equation", *J. Comput. Phys.* **225** (2007) 1533–1552; doi:10.1016/j.jcp.2007.02.001.

[23] R. Mohammadi, "Quintic B-spline collocation approach for solving generalized Black–Scholes equation governing option pricing", *Comput. Math. Appl.* **69** (2015) 777–797; doi:10.1016/j.camwa.2015.02.018.

[24] K. Pal, F. Liu and Y. Yan, "Numerical solutions for fractional differential equations by extrapolation", in: *Finite Difference Methods, Theory and Applications. FDM 2014*, Volume 9045 of *Lect. Notes Comp. Sci*. (eds I. Dimov, I. Faragó and L. Vulkov), (Springer, Cham, 2015) 299–306; https://link.springer.com/chapter/10.1007%2F978-3-319-20239-6_32.

[25] D. Prathumwan and K. Trachoo, "On the solution of two-dimensional fractional Black–Scholes equation for European put option", *Adv. Difference Equ.* **2020** (2020) 146; doi:10.1186/s13662-020-02554-8.

[26] A. Quarteroni, *Numerical Models for Differential Problems*, 2nd edn, Volume 8 of *Modeling, Simulation and Applications* (Springer, Milano, Italy, 2014); doi:10.1007/978-88-470-5522-3.

[27] P. Roul, "A high accuracy numerical method and its convergence for time-fractional Black–Scholes equation governing European options", *Appl. Numer. Math.* **151** (2020) 472–493; doi:10.1016/j.apnum.2019.11.004.

[28] P. Roul, "A fourth order numerical method based on B-spline functions for pricing Asian options", *Comput. Math. Appl.* **80** (2020) 504–521; doi:10.1016/j.camwa.2020.04.001.

[29] P. Roul and V. M. K. P. Goura, "A sixth order numerical method and its convergence for generalised Black–Scholes PDE", *J. Comput. Appl. Math.* **377** (2020) 112881; doi:10.1016/j.cam.2020.112881.

[30] J. Shen, T. Tang and L.-L. Wang, *Spectral Methods. Algorithms, Analysis and Applications*, Volume 41 of *Springer Ser. Comput. Math.* (eds. R. Bank, R. L. Graham, J. Stoer, R. Varga and H. Yserentant), (Springer, Berlin–Heidelberg, 2011); doi:10.1007/978-3-540-71041-7.

[31] L. Song and W. Wang, "Solution of the fractional Black–Scholes option pricing model by finite difference method". *Abstr. Appl. Anal.* **2013** (2013) 194286; doi:10.1155/2013/194286.

[32] W. Wyss, "The fractional Black–Scholes equation", *Fract. Calc. Appl. Anal.* **3** (2000) 51–61.

[33] Y. Xing and Y. Yan, "A higher order numerical method for time fractional partial differential equations with nonsmooth data", *J. Comput. Phys.* **357** (2018) 305–323; doi:10.1016/j.jcp.2017.12.035.

[34] Y. Yan, M. Khan and N. J. Ford, "An analysis of the modified L1 scheme for time-fractional partial differential equations with nonsmooth data", *SIAM J. Numer. Anal.* **56** (2018) 210–227; doi:10.1137/16M1094257.

[35] Y. Yan, K. Pal and N. J. Ford, "Higher order numerical methods for solving fractional differential equations", *BIT* **54** (2014) 555–584; doi:10.1007/s10543-013-0443-3.

[36] T. Yue, "Spectral element method for pricing European options and their Greeks", Dissertation, Duke University, 2012, available at https://hdl.handle.net/10161/6156.

[37] H. Zhang, F. Liu, S. Chen, V. Anh and J. Chen, "Fast numerical simulation of a new time-space fractional option pricing model governing European call option", *Appl. Math. Comput.* **339** (2018) 186–198; doi:10.1016/j.amc.2018.06.030.

[38] H. Zhang, F. Liu, I. Turner and Q. Yang, "Numerical solution of the time fractional Black–Scholes model governing European options", *Comput. Math. Appl.* **71** (2016) 1772–1783; doi:10.1016/j.camwa.2016.02.007.